Available online at www.sciencedirect.com
SCIENCE DIRECT®
Agricultural and Forest Meteorology 132 (2005) 1–19
AGRICULTURAL AND FOREST METEOROLOGY
www.elsevier.com/locate/agrformet

Seasonal dynamics and partitioning of isotopic CO_2 exchange in a C_3/C_4 managed ecosystem

T.J. Griffis [a,*], J.M. Baker [a,b], J. Zhang [a]

[a] *Department of Soil, Water, and Climate, University of Minnesota-Twin Cities, Borlaug Hall, 1991 Upper Buford Circle, St. Paul, MN 55108, USA*
[b] *USDA-ARS, St. Paul, MN, USA*

Received 8 March 2005; accepted 10 June 2005

Abstract

Ecosystem-atmosphere fluxes of $^{12}CO_2$ and $^{13}CO_2$ are needed to better understand the impacts of climate and land use change on ecosystem respiration (F_R), net ecosystem CO_2 exchange (F_N), and canopy-scale photosynthetic discrimination (Δ). We combined micrometeorological and stable isotope techniques to quantify isotopic fluxes of $^{12}CO_2$ and $^{13}CO_2$ over a corn–soybean rotation ecosystem in the Upper Midwest United States. Results are reported for a 192-day period during the corn (C_4) phase of the 2003 growing season. The isotopomer flux ratio, $d^{13}CO_2/d^{12}CO_2$, was measured continuously using a tunable diode laser (TDL) and gradient technique to quantify the isotope ratios of F_R (δ_R) and F_N (δ_N). Prior to leaf emergence δ_R was approximately −26‰. It increased rapidly following leaf emergence and reached an average value of −12.5‰ at full canopy. δ_R decreased to pre-emergence values following senescence. δ_N also showed strong seasonal variation and during the main growing period averaged −11.6‰. δ_R and δ_N values were used in a modified flux partitioning approach to estimate canopy-scale Δ and the isotope ratio of photosynthetically assimilated CO_2 (δ_P) independent of calculating canopy conductance or assuming leaf-scale discrimination factors. The results showed substantial day-to-day variation in Δ with an average value of 4.0‰. This flux-based estimate of Δ was approximately 6‰ lower than the Keeling mixing model estimate and in better agreement with leaf-level observations. These data were used to help constrain and partition F_R into its autotrophic (F_{Ra}) and heterotrophic (F_{Rh}) components based on the numerical optimization of a mass balance model. On average F_{Ra} accounted for 44% of growing season F_R and reached a maximum of 59% during peak growth. The isotope ratio of F_{Rh} (δ_{Rh}), was −26‰ prior to leaf emergence, and became increasingly ^{13}C enriched as the canopy developed indicating that recent photosynthate became the dominant substrate for microbial activity. Sensitivity analyses substantiated that F_{Rh} had a major influence on the seasonal pattern of δ_R, δ_N and the isotopic disequilibrium of the ecosystem. These data and parameter estimates are critical for validating and constraining the parameterization of land surface schemes and inverse models that aim to estimate regional carbon sinks and sources and interpreting changes in the atmospheric signal of $\delta^{13}CO_2$.

Keywords: Net ecosystem exchange; Ecosystem respiration; Stable isotopes; Photosynthetic discrimination; Isotopic disequilibrium; Land use change; Micrometeorology; Flux partitioning

* Corresponding author. Tel.: +1 612 625 3117; fax: +1 612 625 2208.
E-mail address: tgriffis@umn.edu (T.J. Griffis).

0168-1923/$ – see front matter © 2005 Elsevier B.V. All rights reserved.
doi:10.1016/j.agrformet.2005.06.005

1. Introduction

It is well recognized that isotopic CO_2 flux measurements between the ecosystem and atmosphere are needed to better constrain regional estimates of net ecosystem CO_2 exchange (F_N) (Lloyd and Farquhar, 1994; Fung et al., 1997; Buchmann et al., 1998; Randerson et al., 2002; Lai et al., 2004) and the partitioning of F_N into gross photosynthesis (F_P) and ecosystem respiration (F_R) (Yakir and Wang, 1996; Bowling et al., 2001). In particular, better estimates of the isotope ratios of F_N (δ_N), F_R (δ_R), and canopy-scale photosynthetic discrimination (Δ) against $^{13}CO_2$ are needed to improve our current understanding of the global carbon cycle and its sensitivity to climate variation and land use change. The need for improved isotope exchange studies at the ecosystem scale has been highlighted by Fung et al. (1997) who demonstrated that a 3‰ overestimate of Δ in carbon cycle inversion models could result in an underestimate of 0.7 Gt C y^{-1} in the terrestrial carbon sink.

Canopy-scale photosynthetic discrimination is often approximated from the mixing model, $\Delta_b = \delta^{13}C_a - \delta_R$, independent of direct flux measurements (Flanagan et al., 1996; Bakwin et al., 1998). In the above equation, $\delta^{13}C_a$ is defined as the isotope ratio of CO_2 in the surface layer and δ_R is obtained from a Keeling plot (Keeling, 1958). Using a similar definition, Buchmann et al. (1998) defined the parameter ecosystem discrimination, $\Delta_e = (\delta^{13}C_a - \delta_R)/(1 + \delta_R)$, with $\delta^{13}C_a$ referenced with respect to the free atmosphere, to infer changes in ecosystem discrimination caused by photosynthesis. Ideally, these estimates could be used as a suitable surrogate for Δ (Yakir and Sternberg, 2000). However, if an ecosystem is not in isotopic equilibrium (i.e. the isotope ratio of photosynthesis (δ_P) $\neq$ isotope ratio of ecosystem respiration (δ_R)), this approach cannot be expected to yield the true physiological Δ. For instance, Buchmann and Ehleringer (1998) found that Δ_e was 13.2‰ for an alfalfa (*Medicago sativa* L.) C_3 canopy and 13.8‰ for a C_4 corn (*Zea mays* L.) canopy. Contrary to observations from leaf-level experiments, weaker C_4 discrimination (~4‰) was not observed when using this mixing model approach—illustrating the strong influence of land use history on δ_R and the approximation of Δ. Consequently, the above approaches may not provide the best parameterization for regional carbon models because disequilibrium is likely to be the norm as a result of seasonal climate variation, changes in phenology, historical differences in the isotopic composition of soil organic matter and disturbance factors related to land use change. The example above describes an extreme case, yet it highlights the need for a more mechanistic approach, especially when considering that managed agricultural ecosystems represent 12% of the land surface—an area approximately the size of South America (Leff et al., 2004). Furthermore, agricultural ecosystems are highly productive and can, therefore, have a significant influence on ecosystem-atmosphere CO_2 exchange.

Quantifying the isotope ratio of F_R (δ_R) has been the subject of numerous studies (Keeling, 1958; Flanagan et al., 1999; Pataki et al., 2003; Griffis et al., 2004a). Flask-based measurements and the Keeling mixing model have been used as an effective tool to estimate δ_R for a broad range of ecosystems represented in carbon cycle inversion models. Bowling et al. (2002) examined the seasonal variation in δ_R among six coniferous forests over a period of 3 years. Significant differences in δ_R were observed among the forest types, ranging from −33.1 to −23.1‰. Pronounced seasonal variation in δ_R was observed at only the Douglas fir (*Pseudotsuga menziesii*) stand, ranging from −33.0 to −24.5‰. This strong variation was linked to changes in the isotope ratio of assimilated CO_2 in response to changing stomatal conductance caused by precipitation events and variations in vapor pressure deficit. Ometto et al. (2002) also examined seasonal variation in δ_R in forest and pasture ecosystems in the Amazon Basin of Brazil. Seasonal variation in δ_R was minimal at their Manaus forest site, but varied significantly (−29 to −26‰) at the Santarém forest, which experienced strong variations in precipitation. In pastures that replaced clear cut forests, δ_R was enriched by 10‰ and showed strong variation following fire events. In agricultural ecosystems, δ_R values for corn (*Z. mays*) have been reported as −21.6‰ (Buchmann and Ehleringer, 1998) and −20.0‰ (Yakir and Wang, 1996). These values reveal the influence of C_3 crop production in previous years. The differences in δ_R among sites result from the complex interaction of land use history and physiological response to climatic variations. Studies have begun examining the short-term variation in δ_R and its coupling to recently assimilated CO_2 (McDowell et al.,

2004; Knohl et al., 2005; Barbour et al., 2005). Higher sampling frequency, using a flux-based approach, might well reveal greater temporal variation in δ_R and provide a better opportunity to examine how autotrophic (F_{Ra}) and heterotrophic (F_{Rh}) respiration are coupled to changes in F_P.

To this point there have been few flux-based isotopic studies that constrain canopy-scale Δ via flux partitioning (Bowling et al., 2001; Ogée et al., 2003; Lai et al., 2003) and there are insufficient data to permit in depth time series analyses of the behavior of Δ or δ_R at the ecosystem scale. Thus, seasonal and interannual dynamics of these important biophysical parameters remain poorly understood. Moreover, there is significantly less known regarding the behavior of δ_N, because it is extremely challenging to measure directly. The δ_N signal contains valuable information related to the flux weighted sum of ecosystem discrimination factors including: diffusion of CO_2 in free air and laminar boundary layers; equilibrium discrimination of CO_2 entering solution; enzymatic discrimination; discrimination factors related to autotrophic and heterotrophic respiration processes. Bowling et al. (1999, 2001) used relaxed eddy accumulation of CO_2 in flasks and a Keeling transfer function approach (*isoflux* method) to estimate the isotope ratio of F_N (the approximate $^{13}CO_2$ flux). While this innovative approach is being deployed at a number of research sites, to date there have been only five published studies (Bowling et al., 1999, 2001, 2003a; Ogée et al., 2003; Lai et al., 2003) that quantify the $^{13}CO_2$ isoflux. The majority of these studies have been limited in duration to a few weeks or less. Direct flux measurements of δ_N are needed to (1) partition daytime F_N into its gross components (F_R, F_P, F_{Ra}, F_{Rh}); (2) provide important information related to land use change and its impact on the composition of atmospheric CO_2; (3) derive flux-based estimates of Δ and δ_R; (4) provide a top-down constraint on model estimates of ecosystem-discrimination processes.

Recent advances in stable isotope techniques and their combination with micrometeorological methods have provided a means to obtain greater process information and an ability to address some of the problems introduced above. For example, recent developments in tunable diode laser (TDL) technology have provided a methodology suitable for continuous long-term measurements of $^{12}CO_2$ and $^{13}CO_2$ isotopomer mixing ratios (Bowling et al., 2003b). This provides an opportunity for long-term continuous observations of isotopic CO_2 exchange at the field-scale and provides a new tool to improve our understanding of CO_2 cycling dynamics. Specifically, it is now possible to measure the isotopic fluxes, $^{13}CO_2$ and $^{12}CO_2$, of F_N and F_R directly (Griffis et al., 2004a). Therefore, δ_N and δ_R can be obtained from the ratio of the flux measurements, which should provide better estimates of Δ for inversion modeling, partitioning of F_N, understanding the impacts of land use change on CO_2 cycling, and validation of ecosystem models that explicitly account for isotopic fluxes (Fung et al., 1997; Flanagan and Ehleringer, 1998; Yakir and Sternberg, 2000; Riley et al., 2002).

The objectives of this paper are, therefore, to (1) quantify the seasonal changes in canopy-scale photosynthetic discrimination (Δ) and the isotope ratios of F_R (δ_R), F_N (δ_N) and F_P (δ_P) in a corn (C_4)–soybean (C_3) ecosystem in the Upper Midwest using a flux-based approach; (2) partition F_R into its autotrophic (F_{Ra}) and heterotrophic (F_{Rh}) contributions; (3) evaluate the sensitivity of δ_N to changes in F_P, F_{Ra}, and F_{Rh} to better understand how land use change impacts ecosystem-atmosphere isotopic exchange and the extent of isotopic disequilibrium between F_P and F_R.

2. Methodology

2.1. Study site

Field research was conducted at the University of Minnesota Rosemount Research and Outreach Center (RROC), located approximately 20 km south of the St. Paul campus (44°42′N 93°05′W). Micrometeorological and stable isotope measurements were made in a large homogeneous agricultural field. The soil is a Waukegan silt loam (fine, mixed, mesic typic hapludoll), with a surface layer of high organic carbon content (2.6% average) and variable thickness (0.3–2.0 m) underlain by coarse outwash sand and gravel. The field site has been in agricultural production for at least 125 years. The pre-settlement vegetation history for the region is upland dry prairie with dominant plant species consisting of big bluestem (*Andropogon gerardii Vitman*) and Indian grass (*Sorghastrum nutans*) (Marschner, 1974). According to census data records,

our field site was in wheat (C_3 photosynthetic pathway) production as early as 1879 (Minnesota State Agricultural Census Data, Dakota County Historical Society). Field production and management for the last 6 years is summarized as follows: from 1998 to 2001 the field was in continuous corn (*Z. mays* L., C_4 photosynthetic pathway) production; in 2002 the field was planted with soybean (*Glycine max*, C_3 photosynthetic pathway); corn was planted into the field on 2 May 2003. The management scenario is typical of the Upper Midwest with tillage consisting of combination chisel plow/tandem disk and fertilization as dictated by soil tests. A strong isotopic disequilibrium is anticipated for each phase of the rotation given the expected differences between photosynthetic discrimination and the isotope ratio of ecosystem respiration.

Here, we report on simultaneous CO_2 stable isotopomer and EC flux measurements for a 192-day period, 14 May (DOY 134) to 21 November (DOY 325). A few short interruptions in the data resulted from equipment failure and field management activities. Continuous measurements are ongoing as part of the AmeriFlux network.

2.2. Tunable diode laser system

The stable isotopomers, $^{12}CO_2$ and $^{13}CO_2$, were measured using a TDL (TGA100, Campbell Scientific, Logan, UT, USA). A detailed discussion of the methodology can be found in Bowling et al. (2003a, b), Griffis et al. (2004a) and Lee et al. (2005). Briefly, mixing ratios of $^{12}CO_2$ and $^{13}CO_2$ were measured within and above the canopy. The height of the intakes was adjusted through the season as the canopy developed. Each sample inlet consisted of a Delrin 25 mm filter holder with Teflon filter membranes (A-06623-32 and EW-02916-72, Cole Parmer, IL, USA) followed by a brass critical flow orifice (Model: D-7-BR, O'Keefe Controls Co. Monroe, CT, USA). The canopy intake orifices were later replaced with needle valves (SS-SS4-VH, Swagelok, OH, USA). In each case the flow rate was set to 0.260 l min^{-1} to maintain a TDL sample cell pressure of ~2.0 kPa. Synflex tubing (Synflex Type 1300, formerly known as Dekabon, Aurora, OH, USA) connected the inlets located at a micrometeorological tower to an 8-valve custom manifold and then to a Nafion Dryer (PD-200T-24-SS, Perma Pure Inc., NJ, USA) located just before the TDL. Synflex tubing conducted the air streams back to the TDL instrument trailer located at the edge of the field. Within the trailer, the four sample lines and two calibration gas lines were each connected through sample inlet valves mounted on the manifold to the TDL sample inlet. A rotary vane vacuum pump (RB0021, Busch Inc., Virginia Beach, VA, USA) pulled the sample and calibration gases through the TDL sample cell. The manifold sequentially directed the flow from the selected intake to the analyzer and the unselected intakes to the vacuum pump to maintain a constant flow in each intake.

The TDL software controlled the sampling system. Parameters were set to cycle through the four sample inlets and two calibration standards every two minutes as follows: (1) calibration using ~350 μmol mol^{-1} CO_2 with known isotope ratio; (2) calibration using ~600 μmol mol^{-1} CO_2 with known isotope ratio; (3) measurement of CO_2 mixing ratio above the canopy at a height z_4; (4) measurement of CO_2 mixing ratio above the canopy at height z_3; (5) measurement of CO_2 mixing ratio within the canopy at z_2; (6) measurement of CO_2 mixing ratio within the canopy at z_1. The above-canopy sample inlets (z_3 and z_4) were separated by a vertical distance of 0.65 m and their heights were adjusted in relation to the developing canopy on DOY 189 (7 July, z_3 = 1.7m), DOY 199 (18 July, z_3 = 2.66 m), DOY 209 (28 July, z_3 = 3.0 m) and DOY 225 (13 August, z_3 = 3.2 m). Sample inlets within the canopy were positioned at a height of 1 m. Inlet z_2 was used for performing zero gradient tests and was frequently repositioned. Within each 2-min cycle each sample and calibration inlet was sampled for 20 s. An omit time, the time interval following valve switching when data is not recorded, of 7 s was used to allow pressure equilibration and to prevent bias related to sample cell pressure differences and residual sample air from the previous valve selection (Zhang et al., 2005). Following initial plumbing and leak testing, a zero gradient test was performed by moving the inlets to a common height, to ensure there were no systematic differences in the measured mixing ratios of the sample lines.

Primary calibration standards were obtained from the National Oceanic and Atmospheric Administration-Climate Monitoring and Diagnostics Laboratory (NOAA-CMDL). $\delta^{13}CO_2$ values are reported relative to the Vienna Peedee belemnite (VPDB) scale.

Secondary standards were propagated using the TDL system (Griffis et al., 2004a).

2.3. Micrometeorological and ancillary measurements

Half-hourly block averaged water vapor and CO_2 flux measurements were obtained using a three-dimensional sonic anemometer–thermometer (CSAT3, Campbell Scientific Inc.) and an open path infrared gas analyzer (LI-7500, LI-COR, Lincoln, NE, USA). The height of the CSAT3 and LI-7500 were adjusted in relation to the changing canopy height and positioned near the mid-point of the TDL sample inlets located above the canopy. Half-hourly mean covariances of vertical wind speed with sonic temperature, vapor density, and CO_2 density fluctuations were corrected via simultaneous solution of the equations incorporating the Webb et al. (1980) density corrections and the joint influence of temperature and humidity on sonic-derived temperature (Schotanus et al., 1983). Fluxes associated with weak turbulence (friction velocity, $u_* < 0.1$ m s^{-1}) and high humidity (relative humidity >98%) were filtered from the time series. As a result, approximately 46% of the half-hourly eddy covariance flux data was discarded prior to analysis. Other details regarding the eddy covariance measurements, data processing, and data quality can be found in Baker and Griffis (2005). Supporting measurements included: photosynthetically active radiation (P35, Apogee Instruments Inc., Logan, UT, USA); air temperature (HMP35, Vaisala Inc., MA, USA), and leaf area index (LAI) measured with an AccuPAR hand-held sensor (AccuPAR, Mode PAR-80, Decagon Devices Inc., Pullman, WA, USA).

2.4. Isotopic composition of soil and plant organic matter

δ^{13}C of soil organic matter was measured biweekly at depths of 1, 5, 10, 15, 20, 25, 30 and 35 cm. During November 2003 one set of soil samples was taken down to a depth of 1.90 m. Soil samples were dried at 70 °C until the mass of each sample became stable. Samples were sieved at 2 mm and then ground with a ball mill (5300 Mixer/Mill, Spex Industries, Edison, NJ, USA) to a fine powder. δ^{13}C canopy profiles of leaf organic matter were also obtained. Upper-canopy (full sun) and lower-canopy (shade) leaves were sampled and dried at 70 °C for 48 h and ground with the ball mill to a fine powder for stable isotope analysis. Subsamples of approximately 2 and 18 mg for plant and soil matter, respectively, were weighed into foil capsules and processed in duplicate on an elemental analyzer (NA 1500 CHN Analyzer, Carlo Erba, Milan, Italy) interfaced with a continuous flow stable isotope ratio mass spectrometer (Optima, Waters Corporation, Milford, MA). δ^{13}C of soil and plant organic matter are expressed relative to $R_{\text{PDB-Chicago}}$ (i.e. $R_{\text{PDB}} = 0.0112372$) standard ratio.

2.5. Isotopic composition of ecosystem respiration and net ecosystem CO_2 exchange

In this investigation we used the isotopomer flux ratio (Griffis et al., 2004a) method to quantify the seasonal variation in δ_R. Briefly, δ_R is obtained from the ratio of the isotopomer fluxes, which is expressed via K-theory as

$$\frac{F_N^{13}}{F_N^{12}} = \frac{-K_C \overline{\rho}_a / M_a \, \mathrm{d}^{13}\overline{CO}_2/\mathrm{d}z}{-K_C \overline{\rho}_a / M_a \, \mathrm{d}^{12}\overline{CO}_2/\mathrm{d}z} \quad (1)$$

where F_N^{13} and F_N^{12} are the $^{13}CO_2$ and $^{12}CO_2$ fluxes, K_C the eddy diffusivity of CO_2, $\overline{\rho}_a$ the average density of dry air, M_a the molecular weight of dry air, and $\mathrm{d}^{13}\overline{CO}_2/\mathrm{d}z$, $\mathrm{d}^{12}\overline{CO}_2/\mathrm{d}z$ are the time-averaged mixing ratio gradients of $^{13}CO_2$ and $^{12}CO_2$ measured simultaneously at the same heights. Assuming similarity in the eddy diffusivity for $^{12}CO_2$ and $^{13}CO_2$, the flux ratio reduces to $\mathrm{d}^{13}CO_2/\mathrm{d}^{12}CO_2$ and is determined from a geometric linear fit (type II regression) to reduce the influence of outliers. The slope of the regression represents the absolute isotope ratio of F_N. In the absence of photosynthetic activity (nighttime or non-growing season conditions) the regression slope represents the isotope ratio of F_R and is converted to familiar delta notation using:

$$\delta_R = \left(\frac{\mathrm{d}^{13}CO_2/\mathrm{d}^{12}CO_2}{R_{\text{VPDB}}} - 1 \right) \times 10^3. \quad (2)$$

The slope ($\mathrm{d}^{13}CO_2/\mathrm{d}^{12}CO_2$) was obtained from the fit of the 2-min cycle TDL observations for each nighttime (2200–0400 h local time) period (the n value for each fit was approximately 200). Similarly, δ_N was obtained from the flux ratio method for growing

season daytime (0800–1800 h local time) conditions. δ_R and δ_N values were rejected from the analysis when the coefficient of determination (r^2) of the geometric linear fit was less than 0.995. One advantage of the flux ratio method is that it ensures that δ_R and δ_N are consistent with the flux footprint of F_N and it is less susceptible to problems related to advection and extended concentration footprints that occur under stable atmospheric conditions. Lai et al. (2003) demonstrated that some of the seasonal variation in δ_R observed with flask measurements at their tall grass prairie site, near Manhattan Kansas, could be attributed to changes in wind direction and advection from adjacent ecosystems.

δ_R was extrapolated to the daytime based on the assumption that it does not vary significantly on short timescales (<1 day). There has been considerable debate in the recent literature regarding this assumption and it has major implications for isotopic partitioning of F_N and F_R. Lin and Ehleringer (1997) demonstrated that there was no significant discrimination associated with leaf mesophyll respiration while Duranceau et al. (1999) and Ghashghaie et al. (2001) reported significant isotope differences (^{13}C enrichment) of leaf-respired CO_2 compared to leaf substrates in a variety of C_3 plants. Klumpp et al. (2005) recently substantiated the work of Duranceau and Ghashghaie by studying discrimination in respiration at the shoot level. Their work also identified a significant compensating effect (^{13}C depletion) related to discrimination in root respiration. They concluded that the discrimination related to total plant (autotrophic) respiration was very small—resulting in a net ^{13}C enrichment of respiration by 0.7‰. Discrimination related to microbial respiration has also been the subject of similar debate. Henn and Chapela (2000) provide an interesting example showing that fungi (*C. volvatus*, *M. androsaceus* and *S. granulatus*) caused enrichment (0.67–4.91‰) in respired CO_2 relative to a C_3-derived sucrose substrate. When the experiment was repeated with a C_4-derived sucrose substrate there was no significant evidence of discrimination. Consequently, fungal discrimination appears to be species and substrate dependent. It is clear from the above studies that discrimination related to respiration is potentially important, but likely to be less significant than photosynthesis at the ecosystem scale. δ_R will vary depending on the isotope ratio of the substrates consumed during respiration and this does produce short-term fluctuations. For example, Zhang et al. (2005) used the flux ratio method and observed nighttime half-hourly variations in δ_R, which were typically less than 2‰ at the RROC site. Unfortunately, this short-term variation between day and night is likely to cause some instances when our methodological approach results in daytime isotopic mass balances that are not conserved. However, when isotopic disequilibrium is relatively large, flux ratio measurements during the day and night should provide a useful constraint on isotopic flux partitioning and discrimination processes.

2.6. Canopy-scale photosynthetic discrimination

Canopy-scale photosynthetic discrimination, Δ (expressed as a positive value), was approximated using a modified flux partitioning approach based on the conservation of $^{13}CO_2$ (Yakir and Wang, 1996; Bowling et al., 2001; Lai et al., 2003; Zhang et al., 2005). To obtain daytime average values of Δ, independent of canopy conductance (g_c) and independent of leaf-level assumptions related to enzymatic and diffusional discrimination factors, we solved Δ from

$$\delta_N F_N = (\delta^{13}C_a - \Delta)F_P + \delta_R F_R. \quad (3)$$

Eq. (3) was solved using daily values. We make the assumption that F_P and F_R can be obtained from the traditional micrometeorological approach (Black et al., 1996; Goulden et al., 1997; Barr et al., 2002), using nighttime observations (i.e. nighttime $F_N = F_R$) for well mixed conditions ($u_* > 0.1$ m s^{-1}) and estimating daytime gross ecosystem photosynthesis (i.e. $F_P = F_N - F_R$) so that Δ and the isotope ratio of F_P (i.e. $\delta_p = \delta^{13}C_a - \Delta$) can be obtained. Lai et al. (2004) have taken a similar approach, but estimated δ_N from a mixing model. Nevertheless, this method avoids the uncertainties associated with estimating canopy conductance, which is not a trivial matter (Raupach and Finnigan, 1998; Wang and Leuning, 1998; Price and Black, 1990) and avoids the need to scale discrimination factors (i.e. physical diffusion, enzymatic discrimination caused by RuP_2 carboxylation and PEP carboxylase) from the leaf to canopy scale. Leaf-level properties are often scaled to the

canopy based on total LAI or a proportional change in photosynthetically active radiation through the canopy, which can be related to the canopy leaf nitrogen distribution (Field and Mooney, 1986; Farquhar et al., 1989; Dang et al., 1997). In most studies, the leaf-level discrimination parameters are simply applied to the entire canopy (Bowling et al., 2001). The method proposed here can be used to constrain these physiologically based methods, which directly incorporate assumptions related to big-leaf canopy conductance and discrimination factors (Bowling et al., 2001; Ogée et al., 2003; Zhang et al., 2005).

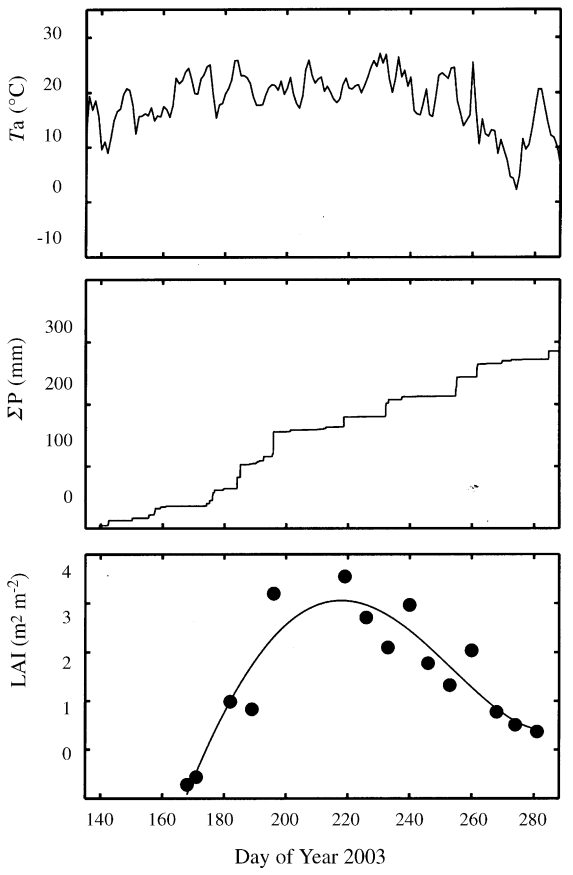

Fig. 1. Climate and phenology at the Rosemount Research and Outreach Center (RRROC) field site during the 2003 growing season. Air temperature (T_a, top panel) was measured above the canopy at the height of the sonic anemometer. Cumulative precipitation ($\sum P$, middle panel) was measured with a tipping bucket rain gauge and leaf area index (LAI, bottom panel) was measured using a leaf area meter and from destructive sampling.

3. Results and discussion

3.1. Climate, phenology and net ecosystem CO_2 exchange

Climatic conditions at the research site were significantly drier (−181 mm) and slightly warmer (+0.3 °C) than the 30-year climate normal (1971–2000 at RROC) from DOY 152 (1 June) through DOY 273 (30 September). Timely precipitation events prevented severe drought and reductions in yield. Total carbon removed during harvest was approximately 470 g C m^{-2} (Baker and Griffis, 2005). Leaf emergence occurred on approximately DOY 163 (12 June). Canopy height reached a maximum of 2.8 m on DOY 210 (29 July). Leaf area index (LAI) attained a maximum value of 4.5 m^2 m^{-2} on DOY 219 (7 August). Leaf senescence showed considerable spatial heterogeneity, likely related to variation in soil depth and soil water content. The majority of the canopy had senesced by DOY 281 (Fig. 1).

Positive F_N, or net loss of CO_2 to the atmosphere, was observed prior to DOY 166. A consistent daytime net CO_2 gain occurred after DOY 166, when LAI had reached 0.25 m^2 m^{-2} (Fig. 2). Nighttime F_R attained a

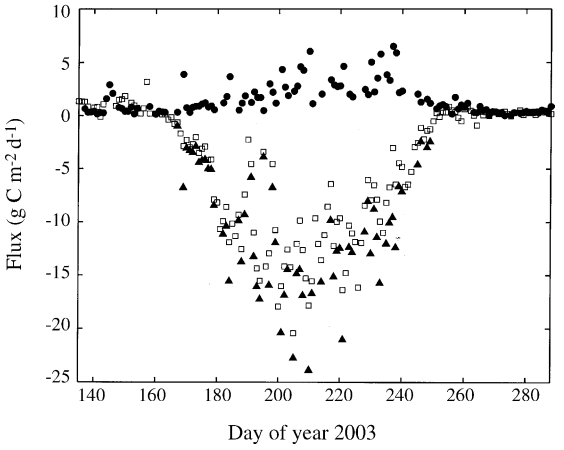

Fig. 2. Seasonal variation of the total daytime net ecosystem CO_2 exchange (F_N, open squares) and total nighttime ecosystem respiration (F_R, closed circles). Gross ecosystem photosynthesis (F_P, closed triangles) was approximated directly by subtracting F_R from daytime F_N. F_N was measured with the eddy covariance technique. Values are shown for $u_* > 0.1$ m s^{-1} with a minimum number of acceptable half-hourly values, $n > 10$ for each case. Details related to the eddy covariance measurements and flux quality control can be found in Baker and Griffis (2005).

maximum of about 6.5 g C m^{-2} d^{-1} from DOY 210 to 238. However, large day-to-day fluctuations were observed. Daytime net CO_2 gain reached a maximum of 20 g C m^{-2} d^{-1} from DOY 200 to 210. F_P reached a maximum of 24 g C m^{-2} d^{-1} on DOY 210. Strong reductions in nighttime F_R, daytime F_N, and F_P were correlated, and occurred during exceptionally dry periods. Two pronounced periods are evident near DOY 213 and 216. Cumulative F_N for the corn phase of the rotation was ~ -390 g C m^{-2} y^{-1} (Baker and Griffis, 2005).

3.2. Isotopic composition of soil and plant organic matter

$\delta^{13}C$ of the soil organic matter indicated that the upper 35 cm was relatively well mixed with no statistically significant trend in $\delta^{13}C$ (Table 1). At a depth below 45 cm the soil organic matter became relatively more enriched. The increased enrichment is likely related to the soil carbon that had accumulated prior to the conversion to agriculture when the area was dominated by C_4 prairie vegetation. Furthermore, deeper soil carbon is expected to be enriched because of the relatively higher lignin content of older soil organic matter (Ehleringer et al., 2000). Canopy $\delta^{13}C$ profiles demonstrated that the top (sunlit) leaves were consistently more enriched compared to the lower (shaded) leaves through the growing season. Both the sunlit and shaded leaves indicated increased relative $^{13}CO_2$ depletion as the growing season progressed. These observations are likely the result of the cumulative effects of recycling/re-fixation of relatively depleted $^{13}CO_2$ air from soil respiration. Compared to the soil samples, the isotope ratios of the leaves were relatively enriched in $^{13}CO_2$ by approximately 6‰.

Table 1
Isotopic composition of soil and plant leaf organic matter measured during the 2003 field season at the Rosemount Research and Outreach Center of the University of Minnesota

(a) $\delta^{13}C$ analysis of soil organic matter[a]

Soil depth (cm)	26 June	29 July	1 October	10 November	Average
1	−17.7 (±0.05)	−17.8 (±0.55)	−19.2 (±0.98)	[b]	−18.2
5	−18.1 (±0.52)	−17.4 (±0.16)	−18.5 (±0.83)	[b]	−18.0
10	−17.5 (±0.49)	−17.3 (±0.26)	−17.9 (±0.96)	[b]	−17.6
15	−16.5 (±1.82)	−17.4 (±0.26)	−18.1 (±0.68)	[b]	−17.3
20	−17.6 (±1.19)	−17.6 (±0.73)	−18.0 (±0.80)	[b]	−17.7
25	−17.4 (±1.00)	−17.2 (±0.20)	−17.7 (±0.42)	[b]	−17.4
30	−18.1 (±0.52)	−17.5 (±0.21)	−16.9[c]	[b]	−17.5
35	−19.0 (±2.31)	−17.2 (±0.56)	−17.8[c]	[b]	−18.0
45	[b]	[b]	[b]	−15.4[c]	
75	[b]	[b]	[b]	−15.3 (±1.98)	
90	[b]	[b]	[b]	−15.1 (±1.87)	
105	[b]	[b]	[b]	−13.2 (±1.83)	
Average	−17.7	−17.4	−18.0	−14.8	−17.7

(b) $\delta^{13}C$ analysis of leaf organic matter[d]

Leaf position	June	July	August	September	Average
Top of canopy	−11.3 (±0.47)	−11.5 (±0.38)	−11.6 (±0.63)	−12.7 (±0.19)	−11.8
Bottom of canopy	−12.0 (±0.22)	−12.1 (±0.52)	−12.3 (±0.41)	[b]	−12.2
Average	−11.7	−11.8	−12.0		−12.0

All isotope ratio values are expressed in dimensionless delta notation (‰, per mil) and are reported relative to Peedee belemnite ($R_{PDB\text{-}Chicago} = 0.0112372$).

[a] Terms in parentheses indicate the standard deviation of three samples taken from different soil cores.

[b] Samples not available.

[c] Only one sample available.

[d] Terms in parentheses indicate the standard deviation of 16 samples taken from different plants.

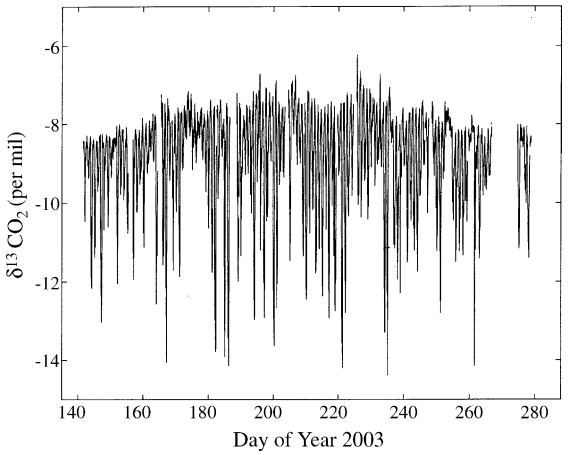

Fig. 3. Seasonal variation of the isotope ratio of CO_2 ($\delta^{13}CO_2$) measured above the developing corn canopy during the 2003 growing season. Half-hourly values are based on the average of 15 2-min TDL measurement cycles.

3.3. Variations of $\delta^{13}CO_2$ in the surface layer

Half-hourly variations of $\delta^{13}CO_2$ showed a distinct diurnal and seasonal pattern (Fig. 3). Throughout the year during stable nighttime conditions the accumulation of CO_2 in the surface layer resulted in large negative $\delta^{13}CO_2$ values, often less than −12‰. From DOY 140 to 160 (late May to early June) the surface layer was relatively depleted in $^{13}CO_2$ due to the accumulation of respired CO_2. During the early spring and late fall the $\delta^{13}CO_2$ of the well-mixed ($u_* > 0.1$ m s^{-1}) surface layer was approximately −8.5‰. Following leaf emergence, daytime F_P caused the surface layer to become relatively enriched in $^{13}CO_2$. When atmospheric mixing was strong, $\delta^{13}CO_2$ was higher than −8.0‰, reaching a maximum value of −6.3‰ during early August (DOY 225). The enrichment was caused by F_P and the entrainment of relatively clean air from above the surface layer. The onset of senescence is evident after DOY 250 as the daytime $\delta^{13}CO_2$ decreased back to values similar to early spring due to a diminution in the preferential removal of $^{12}CO_2$ by F_P. Two periods during the growing season provide anecdotal evidence that the dry summertime conditions reduced F_P as the daytime $\delta^{13}CO_2$ values became less enriched in $^{13}CO_2$. Most evident is the period DOY 213–220 (1–8 August). Rain on DOY 218 enhanced F_P and caused a significant enrichment in the $\delta^{13}CO_2$ to about −6.9‰.

Fig. 4 shows the diurnal pattern of $\delta^{13}CO_2$ and F_N during three periods including: pre-leaf to early leaf

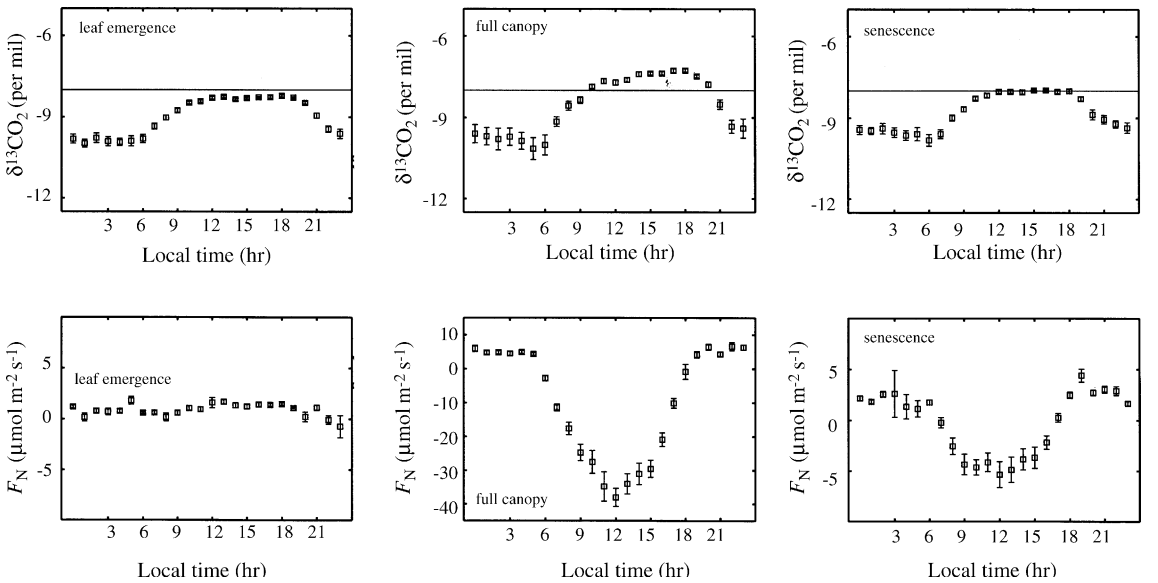

Fig. 4. Typical diurnal patterns of net ecosystem CO_2 exchange and the isotope ratio, $\delta^{13}CO_2$, measured above the developing corn canopy during three different growing periods in 2003 including: pre-leaf emergence (DOY 135–168; 15 May–17 June, left-hand panels), peak canopy growth (DOY 195–207; 14 July–26 July, middle panels) and onset of canopy senescence (DOY 240–257; 28 August–14 September, right-hand panels). A $\delta^{13}CO_2$ value of −8‰ is shown by the solid horizontal line in the upper panels for reference.

emergence (DOY 135–168; 15 May–17 June); peak canopy growth (DOY 195–207; 14–26 July) and onset of senescence (DOY 240–257; 28 August–14 September). Each plot illustrates the influence of the stable nocturnal boundary layer and the transition to a daytime well-mixed unstable surface layer. Nocturnal $\delta^{13}CO_2$ values were typically less than −9‰. The upper left-hand panel of Fig. 4 shows the diurnal amplitude of $\delta^{13}CO_2$ during a period when daytime F_N and nighttime F_R were approximately equal (lower left panel) and indicates that boundary layer dynamics alone account for a diurnal amplitude variation of at least 1.5‰. During the peak growing season (upper middle panel), daytime enrichment of atmospheric $\delta^{13}CO_2$ reached a maximum at 1800 h local time, which lagged the maximum observed F_N (lower middle panel) by about 6 h. This maximum for $\delta^{13}CO_2$ was related to the expansion of the planetary boundary layer and the cumulative effects of biological discrimination. The diurnal $\delta^{13}CO_2$ amplitude increased to about 3.0‰ during this period as a result of increased biological $^{13}CO_2$ discrimination. The right-hand panels of Fig. 4 indicate that the boundary layer enrichment of $^{13}CO_2$ and the diurnal amplitude of $\delta^{13}CO_2$ decreased substantially at the onset of senescence.

Fig. 5 shows the variation in surface layer $\delta^{13}CO_2$ as a function of F_N. From early morning to early afternoon, increasing F_P and expansion of the boundary layer resulted in rapid enrichment of the surface layer. The transition from afternoon to early evening showed a strong reduction in net CO_2 gain with little change in $\delta^{13}CO_2$. At night, F_R was relatively constant over a period of about 11 h, while $\delta^{13}CO_2$ rapidly became more depleted as the nocturnal boundary layer developed. The hysteresis loop reveals the effects of cumulative F_N and, more importantly, the strong dependence of surface layer $\delta^{13}CO_2$ on boundary layer dynamics, which have been shown to impart a substantial influence on the estimates of δ_R and Δ_e when using the Keeling approach (Pataki et al., 2003; Lloyd et al., 1996). One important advantage of the flux ratio method is that it eliminates the influence of these boundary layer effects (Griffis et al., 2004a).

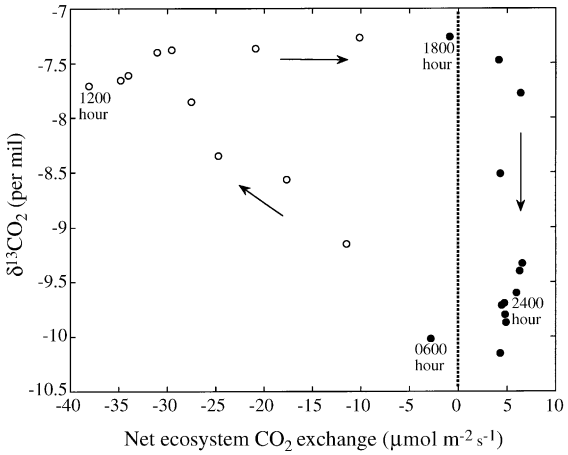

Fig. 5. The relation of surface layer $\delta^{13}CO_2$ to net ecosystem CO_2 exchange. Ensemble data are shown for the peak growing period (DOY 195–207). Arrows indicate the hysteresis loop and the progression of time beginning at 0600 h. Solid symbols represent 1800–0600 h. Open symbols represent 0700–1700 h.

3.4. Isotopic composition of flux components

Previous flux ratio measurements and Keeling plot analyses at this site showed considerable day-to-day variation in the isotope ratio of non-growing season respiration (δ_R) with values characteristic ($\delta_R = -27.9$‰) of C_3 substrates (Griffis et al., 2004a). These initial measurements were conducted over a 26-day period in November 2002 following harvest of soybean when conditions were cold and fluxes relatively small. δ_R values were very similar using both techniques, but errors were considerably larger for the flux ratio approach, presumably due to the difficulty of resolving small isotopomer gradients. In this comparison δ_R was estimated from the flux ratio (Fig. 6 upper right panel) and Keeling method (Fig. 6 upper left panel) using sample inlets located both within and above the canopy. Each method and estimate, shown in Fig. 6, illustrates strong seasonal variation related to the phenology of the developing corn canopy. The degree of correlation between the flux ratio measured within and above the canopy was moderate ($r = 0.74$). Correlation among the two Keeling estimates measured above the canopy was very strong ($r = 0.95$) and was weaker ($r = 0.85$) for the measurement inside the canopy relative to the lowest inlet above the canopy. The lower correlation among δ_R values for within versus above canopy estimates is likely related to the difference in source footprint. Correlation between the flux ratio and the

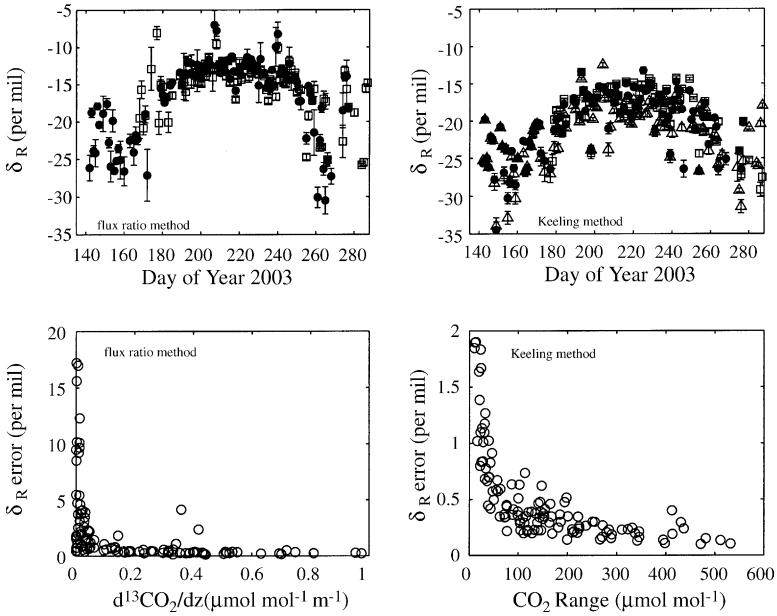

Fig. 6. Seasonal variation in the isotope ratio of ecosystem respiration (δ_R) estimated using the flux ratio (upper left-hand panel) and the Keeling mixing model (upper right-hand panel) approach. The flux ratio was estimated from the $d^{13}CO_2/d^{12}CO_2$ gradient measured above the canopy (closed circles) and within the canopy (open squares). Each data point represents a nighttime value determined from approximately 200 observations. The Keeling estimate was measured within the canopy (z_1, open squares) and above the canopy at two different heights (highest height (z_4, open triangles) above the canopy and lowest height (z_3, closed circles) above the canopy). Each data point represents a nighttime value determined from approximately 200 observations. The lower panels illustrate the sensitivity of the error estimate for each method. The flux ratio error estimate (lower left-hand panel) was large when the $^{13}CO_2$ gradient was less than 0.035 μmol mol m^{-1}. The Keeling error estimate (lower right-hand panel) increased significantly when the nighttime range in CO_2 mixing ratio was less than 80 μmol mol^{-1}.

Keeling δ_R values (measured above the canopy) was good ($r = 0.70$), but weaker than the within-method comparison. For the active growing period, the uncertainty in the estimate of δ_R was greater for the flux ratio (S.E. = ±0.83‰ above canopy; S.E. = ±0.62‰ within canopy) than the Keeling method (S.E. = ±0.65‰). Fig. 6 (lower panels) illustrates the sensitivity of the flux ratio and Keeling methods to the $^{13}CO_2$ gradient and range in total CO_2 mixing ratio, respectively. The standard error of δ_R decreased substantially when the nighttime $^{13}CO_2$ mixing ratio gradient exceeded 0.035 μmol mol^{-1} m^{-1}. Similarly, the Keeling plot estimate of δ_R improved when the range of CO_2 mixing ratio exceeded 80 μmol mol^{-1}. The latter result is in excellent agreement with the findings of Pataki et al. (2003). For ideal conditions (large $^{13}CO_2$ gradient or large range in CO_2 mixing ratio) both methods result in similar error estimates, however, we observed a significant difference between the flux ratio and Keeling δ_R values that tended to increase to a mid-season maximum of about 5‰ and correlated with peak canopy development and photosynthesis. This bias was not observed for non-growing season conditions in 2002 (Griffis et al., 2004a) and was not pronounced during early spring and late fall during 2003. We hypothesize that this growing-season difference was related to the larger footprint of the concentration measurements and the susceptibility of the Keeling method to contamination from combustion plumes. The research site is bordered by other C_3 crops and forests and is also located at the urban/rural interface and, therefore, subject to elevated CO_2 resulting from point source combustion. In this case, advection and contamination problems would be most evident over a C_4 canopy due to the large difference in isotopic end members. Recent oxygen isotope measurements of CO_2 using the TDL method showed Keeling plot intercepts that were characteristic of a combustion signal (Griffis et al., 2005). Given these potential factors, we focus our

analysis on δ_R values obtained from the flux ratio above the canopy.

δ_R fluctuated from about −26 to −18‰ from DOY 140 to 170 (20 May–19 June) and rapidly increased (enriched in $^{13}CO_2$) as the corn canopy developed and F_P increased. During full canopy δ_R varied from about −15 to −11‰. Night-to-night variation in δ_R was approximately ±4‰ and was typically larger than the relative error of the estimate. Further, the night-to-night variation was similar to the within-night variability (6.4‰) observed for an irrigated agricultural crop that had no influence of C_4 vegetation within the last 20 years (Bowling et al., 2003b). δ_R rapidly became more negative as the corn canopy senesced. Large variations were observed during early spring and late fall when CO_2 fluxes were small. The isotope ratio of the soil organic matter (Table 1) illustrates that F_R was in general, relatively enriched in $^{13}CO_2$, compared to the soil organic carbon (even after accounting for the 4.4‰ fractionation related to soil gas diffusion) during the mid growing period. It is well known that the isotope ratio of bulk soil organic matter is a poor predictor of δ_R (Ehleringer et al., 2000). Average (±S.D.) spring (DOY 135–180), mid-summer (DOY 200–230), and fall (DOY 250–280) values of δ_R were −22.0‰ (±3.5‰), −12.5‰ (±1.7‰) and −19.9‰ (±5.5‰), respectively. Variations in δ_R were large during spring and fall, the transition seasons when fluxes are small and temporal changes in soil heat content and temperature distribution with depth are greatest. Unfortunately, a cryocooler failure on the TDL prevented us from examining these variations thoroughly through the winter period. We hypothesize that these large fluctuations were related to changes in respiration associated with shallow soil carbon (recent C_3 soybean origin) versus deep soil (prairie C_4 origin) decomposition and reflect the complexity of a system that has been managed for more than 125 years.

δ_N values varied from −33 to −4‰ (Fig. 7, top panel) over the course of the measurement period and showed a similar seasonal pattern as δ_R, which was related to canopy phenology. The daily fluctuations in δ_N and δ_R, however, were poorly correlated ($r = 0.24$). Spring and fall δ_N values showed large day-to-day variation ranging from −33 to −15‰. During the main growing period (DOY 175–240) δ_N varied from −22 to −4‰ (average of −11.6‰). A robust linear regression technique that minimizes differences in the absolute residuals instead of the squared differences by using a reweighted least squares algorithm (DuMouchel and O'Brien (1989), Matlab V7, The Mathworks Inc., USA) was used to quantify the trend in δ_N for the growing period. The regression analysis indicates that δ_N decreased (i.e. greater relative depletion in $^{13}CO_2$) as the growing season progressed ($\delta_N = -0.021\text{DOY} - 7.11$, $r^2 = 0.62$) from DOY 175 to 240. We note, however, that the slope of the regression is not significantly different from zero at the 0.05 significance level.

Daily estimates of Δ were computed from Eq. (3) using δ_R values obtained from the flux ratio and the Keeling methods (Fig. 7, middle panel). The maximum probable error of Δ was estimated by examining the partial derivatives of Δ with respect to each dependent variable following the error propagation method of Bevington (1969). The error terms included the mean standard error estimates of δ_R and δ_N, a relative error of 25% for the eddy covariance flux measurements (Morgenstern et al., 2004), and an uncertainty of 0.07‰ for $\delta^{13}C_a$ (Griffis et al., 2004a). The estimated maximum probable error for Δ averaged ±1.8‰. The largest source of uncertainty was related to the estimate of δ_N (∼1.5‰) followed by δ_R (∼0.21‰) and F_R (∼0.09‰). Based on the error analysis, the flux ratio estimate of Δ was not significantly different from that computed using the Keeling-derived δ_R values. A recent error propagation study by Ogée et al. (2004) has shown that isotopic flux partitioning and estimates of Δ are subject to large errors when the ecosystem isotopic disequilibrium ($\delta_e = \delta_R - \delta_P$) is small (≤4‰). In this study, δ_e was often less than 2‰ during the mid to late growing period.

Δ varied from about 1–15‰. Significant scatter and unexpected values (>8‰) occurred at the time of leaf emergence and during leaf senescence. During the main growing period Δ varied from 1 to 6‰. The average Δ was 4.0 and 5.2‰, based on the flux ratio and Keeling-derived δ_R values, respectively. Fessenden and Ehleringer (2003) examined monthly changes in leaf-level discrimination and isotope ratios of leaf organic matter in an old growth forest of the Pacific Northwest under a variety of climatic conditions from 1998 to 2000 and did not observe significant seasonal variation in Δ. Baldocchi and Bowling (2003), however, modeled strong diurnal variation in Δ for

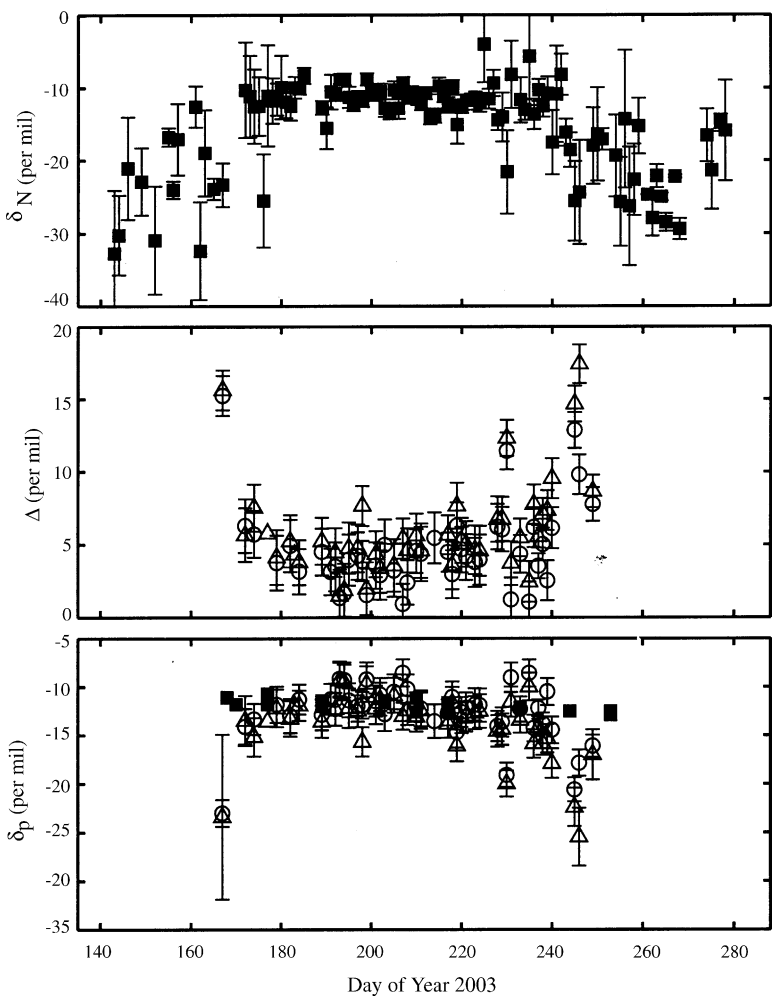

Fig. 7. Seasonal variation in the isotope ratios of net ecosystem CO_2 exchange (δ_N, top panel), canopy-scale discrimination (Δ, middle panel) and photosynthetically assimilated CO_2 (δ_P, bottom panel). Canopy-scale discrimination and the isotope ratios of photosynthetically assimilated CO_2 were estimated from the flux-based approach (Eq. (3)) using δ_R obtained from the flux ratio method (open triangles) and Keeling approach (open circles). Also shown are the isotope ratios of leaf organic matter (closed squares) measured during the growing season. δ_N was measured directly from the daytime flux gradient $d^{13}CO_2/d^{12}CO_2$ using the 2-min TDL data. The δ_N error bars represent the standard error of the estimate. The error bars shown for Δ and δ_P represent the maximum probable error obtained by examining the partial derivatives of Eq. (3) with respect to each independent variable.

a deciduous Tennessee forest with values ranging from 18 to 27‰. Our average growing season Δ values (4.0 ± 1.9‰) were in good agreement with leaf-level discrimination measurements obtained by Vogel (1980) for corn leaves (3.3‰) and modeled values for C_4 plants (3.6‰) estimated by Lloyd and Farquhar (1994). Although the relative error estimates of Δ are large, this experiment represents a rigorous test because the isotopic disequilibrium was relatively small during the mid to late growing period and C_4 discrimination is relatively weak. Our methodology for constraining Δ may have a significant advantage for complex canopies such as prairies (C_3 and C_4 plants), wetlands (vascular and non-vascular plants), or forests (complex overstory and understory) where it can be difficult to define and scale up leaf-level parameter values. We acknowledge that over rougher surfaces, such as forests, we will need to combine the

TDL and eddy covariance method directly to obtain the isotopic fluxes. This has not yet been attempted and remains an important and challenging problem.

The isotope ratio of the assimilated CO_2 (i.e. $\delta_P = \delta^{13}C_a - \Delta$) is shown in Fig. 7 (lower panel). δ_P was calculated using both the flux ratio and Keeling-derived estimates of Δ. Error bars represent the maximum probable error estimated using the procedure described above. During the main growing period δ_P varied from −19 to −9‰. The average δ_P values were −12.7 and −14.0‰ computed from the flux ratio and Keeling-derived δ_R values, respectively. Based on the error analysis these values are not significantly different. There was a weak decreasing trend ($\delta_P = -0.022\text{DOY} - 7.0$, $r^2 = 0.25$) in δ_P for the period DOY 175–240 with slope and intercept nearly identical to those for δ_N (not statistically significant at the 0.05 significance level). Also shown in Fig. 7 are the isotope ratios of the leaf organic matter, which show excellent agreement with δ_P in both magnitude (−12.0‰) and growing season trend/slope. We hypothesize that the decrease in δ_P and δ_N through the main growing season resulted from the recycling/refixation of recently respired CO_2 (Lloyd et al., 1996). We note that values of δ_N were not always bounded by δ_P and δ_R. These instances were likely related to measurement errors or resulted from differences between nighttime δ_R and daytime δ_R causing an isotopic mass balance that was not conserved.

3.5. Flux partitioning, land use change, and isotopic disequilibrium

The rapid increase in δ_R (^{13}C enrichment) as the corn canopy developed indicates that recent CO_2 assimilation by corn was the major substrate for F_R. The shift in a source characteristic of C_3 residue to that of a C_4 corn canopy is driven by autotrophic respiration and the microbial decomposition of fresh residue and exudates. Högberg et al. (2001) have shown that reduced photosynthate supply to roots can reduce soil respiration by about 54%. Rochette et al. (1999) used a mixing model experiment to partition soil respiration into heterotrophic (C_3) and autotrophic (*Z. mays* L., C_4) respiration by planting *Z. mays* into a C_3 soil. They found that 45% of the total soil respiration during the growing season could be attributed to autotrophic respiration. Given the complex land use history at our research site it is very difficult to use a two-end member mixing model to partition F_R into its autotrophic and heterotrophic components. Further, there is substantive evidence that the isotope ratio of soil organic matter is a poor predictor of the isotopic composition of F_R (Ehleringer et al., 2000), making it difficult to combine mass and flux-based methodologies. Here, we partitioned F_R into autotrophic (F_{Ra}) and heterotrophic (F_{Rh}) respiration from the conservation of $^{13}CO_2$ fluxes:

$$\delta_N F_N = \delta_{Ra} F_{Ra} + \delta_{Rh} F_{Rh} + \delta_P F_P \quad (4a)$$

where δ_{Ra} and δ_{Rh} are the isotope ratios of the autotrophic and heterotrophic contributions, respectively. Eq. (4a) was rearranged to retrieve the isotopic signature of F_{Ra}, F_{Rh}, and the fraction of autotrophic respiration (A) from

$$\delta_N F_N = \delta_{Ra} F_R A + \delta_{Rh} F_R (1 - A) + \delta_P F_P. \quad (4b)$$

Daily values of δ_N, F_N, F_R, δ_P and F_P were used to optimize Eq. (4b). The parameters, A, δ_{Rh} and δ_{Ra} were determined at 12-day intervals using the Nelder–Mead simplex (direct search) optimization routine (Matlab V7, The Mathworks Inc., USA). Initial parameters were specified for A, δ_{Rh} and δ_{Ra} as 0.45, −20 and −10‰, respectively without specifying upper or lower bounds on δ_{Rh} or δ_{Ra}.

Fig. 8 (upper left panel) illustrates the quality ($r^2 = 0.54$) of the optimization procedure. Data are shown for approximately 5000 simulations, which involved the random removal of measured input data prior to optimization. Outliers indicate instances when the isotopic mass balance was not conserved, probably because of measurement error or differences in δ_R between daytime and nighttime related to discrimination or substrate availability. The upper right panel of Fig. 8 shows the relationship between predicted and measured δ_R for each time interval and indicates that the F_R flux partitioning and its isotopic composition is in excellent agreement ($r^2 = 0.95$) with observations. The relative contribution of growing season F_{Ra} (Fig. 8, lower left panel) averaged 44% and ranged from about 27% during the early growing season to a maximum of 59% by DOY 195 (14 July). F_{Ra} decreased to about 9% during senescence. The optimized isotopic compositions of F_{Ra} and F_{Rh} are shown in the lower right panel of Fig. 8. δ_{Ra} averaged −10.5‰, showed little variation over the growing period, and was enriched by

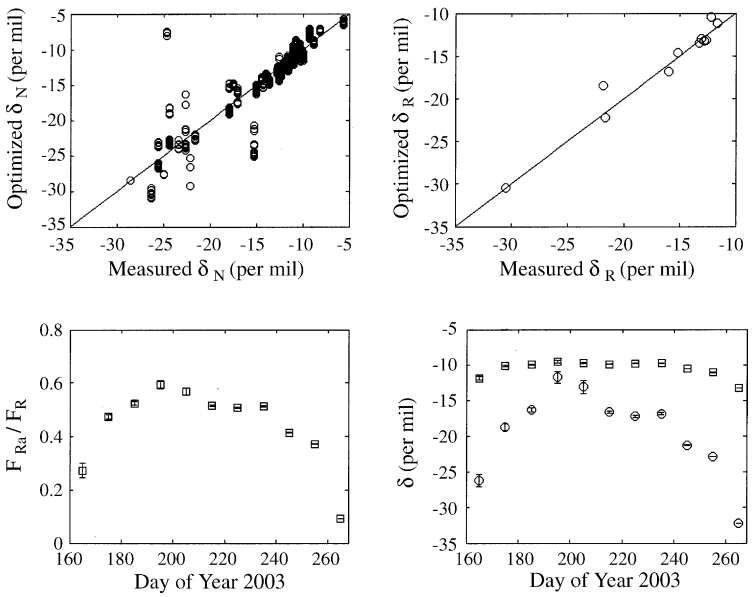

Fig. 8. Constraining autotrophic (F_{Ra}) and heterotrophic (F_{Rh}) respiration and their isotopic composition using a numerical optimization technique. δ_N (upper left-hand panel) was optimized via Eq. (4b) using a Nelder–Mead simplex routine at 12-day intervals. The uncertainty in the optimization procedure was evaluated by randomly removing measured δ_N values from the time series and repeating the optimization routine. This entire procedure was repeated 5000 times to obtain the error bars (S.D.) shown in the lower panels. Measured δ_R was compared to the optimized δ_R as an independent check on the quality of the optimization procedure (upper right-hand panel). The relative contribution of F_{Ra} is shown in the lower left-hand panel. Isotopic compositions of F_{Ra} (open squares) and F_{Rh} (open circles) are shown in the lower right-hand panel.

approximately 2.2‰ relative to δ_P. δ_{Ra} is expected to differ slightly from δ_P because of secondary metabolic processes involved in the biosynthesis of sucrose, starch, cellulose and hemicellulose (^{13}C enriched products) and lipids and lignins (^{13}C depleted products) (Ehleringer et al., 2000). As expected, δ_{Rh} showed strong seasonal variation ranging from −26.2‰ during the early growing period to −11.7‰ during rapid canopy growth. As the canopy senesced, δ_{Rh} decreased to −32.2‰. This analysis highlights that the seasonal variation of δ_R is driven by both the large contribution of F_{Ra} and a shift in microbial activity from the C_3 (soybean residue from the previous year's rotation) to C_4 substrates (fresh root exudates). This also explains the rapid change in δ_R following senescence and provides further evidence that the isotopic analysis of bulk soil organic matter is not a good predictor of δ_R for this particular site. Constraining δ_R from the isotopic analysis of soil organic matter must be limited to the biologically relevant carbon substrates (i.e. water soluble fraction/light-fraction organic matter) that dominate ecosystem respiration. The ability to separate F_R into F_{Ra} and F_{Rh} from the inversion of atmospheric isotopic flux measurements is a potentially powerful tool that could be used to further constrain other approaches based on chamber methodologies (Griffis et al., 2004b).

Sensitivity analysis of the flux partitioning equation (Eq. (4a)) was used to better understand the impact of land use change (i.e. C_3/C_4 crop rotation) on isotopic CO_2 exchange with the atmosphere and to examine the extent of isotopic disequilibrium between F_P and F_R. The conversion from a C_3 to a C_4 ecosystem imposes a step change in Δ and results in a progressive change in δ_R related to the recent assimilation of carbon substrates (fast carbon pool) and the accumulation of soil organic matter (slow carbon pool). Insight into the rate of atmospheric enrichment/depletion (change in δ_N) due to the recently established C_4 canopy was obtained from the partial derivatives of Eq. (4a) with respect to F_P ($\partial\delta_N/\partial F_P = \delta_P/F_N$), F_{Ra} ($\partial\delta_N/\partial F_{Ra} = \delta_{Ra}/F_N$) and F_{Rh} ($\partial\delta_N/\partial F_{Rh} = \delta_{Rh}/F_N$). Initial conditions were

based on early growing season (DOY 165–185) typical values of δ_P, δ_{Ra}, and δ_{Rh} of −11.6, −10.7 and −20.4‰, respectively. Using the data shown in Fig. 2 we calculated sensitivity factors of 2.5, 2.3 and 4.4‰ for F_P, F_{Ra} and F_{Rh}, respectively. The greater sensitivity of δ_N to F_{Rh} emphasizes the importance of carbon released by plant roots, i.e. the most influential cause of seasonal variations of δ_N and δ_R in this system is the preference of soil microbes for fresh root exudates over older soil carbon.

The isotopic disequilibrium (δ_e) between F_P and F_R was greatest at leaf emergence and diminished toward equilibrium as the growing season progressed. Evaluation of the above derivatives during the peak growing season (DOY 205–225) showed similarity and reduced sensitivity, 0.8, 0.7 and 1.0‰, with respect to F_P, F_{Ra} and F_{Rh}, respectively. On DOY 228 isotopic disequilibrium reached a minimum of 0.5‰ and Δ_b was in excellent agreement with the flux-based estimate of Δ (Fig. 9). Unlike methods that approximate Δ from the Keeling mixing model, the flux-based approach does not require the underlying ecosystem to be in isotopic equilibrium in order to provide physiologically meaningful estimates. In our case, agreement between the two methods improved after full canopy development, when near-equilibrium can be expected, but they diverged over much of the growing season, when heterotrophic respiration of C_3 substrates had a larger effect on δ_R and therefore Δ_b. During the main growing period average values of Δ and Δ_b were 4.0 and 10.1‰, respectively.

NOAA-CMDL measurements from the WLEF tower in Wisconsin, USA showed that regional δ_R and Δ_b were approximately −24.7 and 16.8‰, respectively (Bakwin et al., 1998). The tower is located in a region dominated by deciduous forest with relatively little direct urban influence. For a similar ecosystem, Bowling et al. (2001) obtained canopy-scale Δ from leaf-level assumptions in combination with the isotope flux partitioning methodology. They obtained δ_R and Δ values of −24.9 and 17‰ for a deciduous forest in eastern Tennessee. For ecosystems that do not experience major disturbances, the approximations, Δ_e or Δ_b, may provide an adequate solution. Additional comparisons are needed for natural and undisturbed ecosystems in order to better quantify the seasonal variation and extent of isotopic disequilibrium and its impact on the difference between Δ and Δ_b. The difference in these estimates could become of increasing importance due to climate and land use change.

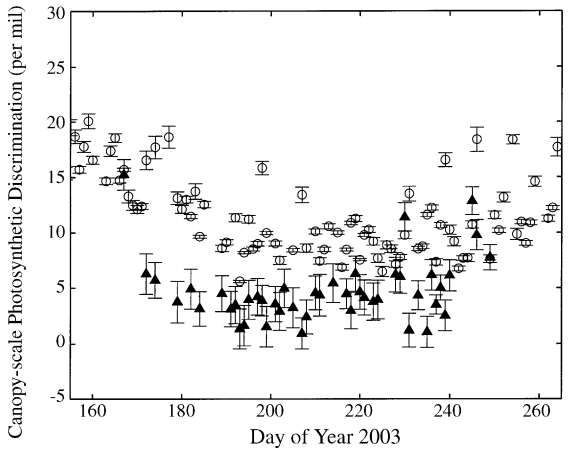

Fig. 9. Seasonal variation of ecosystem discrimination (Δ_b) compared to the flux-based estimate of canopy-scale photosynthetic discrimination (Δ). Δ_b (open circles) was calculated as $\Delta_b = \delta^{13}C_a - \delta_R$, where $\delta^{13}C_a$ is the average isotope ratio of CO_2 measured above the canopy and δ_R is the isotope ratio of ecosystem respiration estimated from the Keeling mixing model approach. The error bars represent the standard error of the Keeling plot intercept. Δ (closed symbols) was approximated from the modified flux partitioning approach via the inversion of Eq. (3). The error bars represent the maximum probable error obtained by examining the partial derivatives of Eq. (3) with respect to each independent variable.

4. Conclusions

1. The flux ratio method was used to quantify the seasonal variation in the isotope ratio of ecosystem respiration (δ_R) and net ecosystem CO_2 exchange (δ_N) in a C_3/C_4 managed agricultural ecosystem for a 192-day period during 2003. Development of the C_4 (corn) canopy resulted in dramatic changes in δ_R and δ_N. δ_R changed rapidly from approximately −26‰ to about −18‰ following leaf emergence. At full canopy δ_R varied between −15 and −11‰ and decreased rapidly at the onset of senescence. δ_N also showed a strong seasonal pattern with values ranging from −33 to −4‰. The seasonal variation of δ_R and δ_N was caused primarily by changes in phenology.

2. Canopy-scale photosynthetic discrimination (Δ) was estimated using a modified flux partitioning approach independent of calculating canopy conductance or making leaf-level assumptions about discrimination factors. At full canopy, Δ varied from 1 to 6‰ and averaged 4.0‰. The estimated isotope ratio of assimilated CO_2 (δ_P) averaged -12.7‰ and was in excellent agreement with the isotopic composition of leaf organic matter.
3. Ecosystem respiration (F_R) was partitioned into its autotrophic (F_{Ra}) and heterotrophic (F_{Rh}) components based on the conservation and numerical optimization of a mass balance model. On average F_{Ra} accounted for 44% of growing season F_R and reached a maximum of 59% during peak growth. The isotope ratio of F_{Ra} (δ_{Ra}) and F_{Rh} (δ_{Rh}) was also retrieved from the optimization routine. δ_{Ra} was relatively enriched compared to δ_P and averaged -10.5‰. δ_{Rh} varied from -26‰ at leaf emergence and progressively became ^{13}C enriched as the canopy developed indicating that recent photosynthate became the dominant substrate for microbial activity. A sensitivity analysis indicated that F_{Rh} had a major influence on the seasonal variation of δ_R, δ_N and isotopic disequilibrium.
4. Isotopic disequilibrium, the difference between δ_p and δ_R, diminished to 0.5‰ during the mid to late growing season. During this period, the mixing model estimate of discrimination, $\Delta_b = \delta^{13}C_a - \delta_R$, was in better agreement with the flux-based estimate of Δ. However, Δ_b over-estimated Δ by about 6‰ for much of the growing season when the isotopic disequilibrium was large.

Acknowledgements

This research was supported by the Office of Science (BER), U.S. Department of Energy, Grant No. DE-FG02-03ER63684 (TJG & JMB). Funding for this project was also provided by the University of Minnesota, Grant-in-aid of Research, Artistry and Scholarship (TJG). The authors would like to thank USDA-ARS technicians Bill Breiter, Martin DuSaire, and Mike Dolan, and undergraduate research assistant, Megan Lennon for their dedicated assistance in the field and laboratory. We thank Xuhui Lee at Yale University for recent discussions related to the flux ratio approach and recognize the helpful technical support of Steve Sargent at Campbell Scientific Inc. Finally, we thank two anonymous reviewers for their critical comments and helpful suggestions.

References

Baker, J.M., Griffis, T.J., 2005. Examining strategies to improve the carbon balance of corn/soybean agriculture using eddy covariance and mass balance techniques. Agric. Forest Meteorol. 128, 163–177.

Bakwin, P.S., Tans, P.P., White, J.W.C., Andres, R.J., 1998. Determination of the isotopic (C-13/C-12) discrimination by terrestrial biology from a global network of observations. Global Biogeochem. Cycles 12 (3), 555–562.

Baldocchi, D.D., Bowling, D.R., 2003. Modelling the discrimination of (CO_2)-C-13 above and within a temperate broad-leaved forest canopy on hourly to seasonal time scales. Plant Cell Environ. 26 (2), 231–244.

Barbour, M.M., Hunt, J.E., Dungan, R.J., Turnbull, M.H., Brailsford, G.W., Farquhar, G.D., Whitehead, D., 2005. Variation in the degree of coupling between $\delta^{13}C$ of phloem sap and ecosystem respiration in two mature Nothofagus forests. New Phytologist. doi:10.1111/j.1469-8137.2005.01329.x.

Barr, A.G., Griffis, T.J., Black, T.A., Lee, X., Staebler, R.M., Fuentes, J.D., Chen, Z., Morgenstern, K., 2002. Comparing the carbon budgets of boreal and temperate deciduous forest stands. Can. J. Forest Res. (Revue Canadienne de Recherche Forestiere) 32 (5), 813–822.

Bevington, P.R., 1969. Data Reduction and Error Analysis for the Physical Sciences. McGraw-Hill, New York.

Black, T.A., DenHartog, G., Neumann, H.H., Blanken, P.D., Yang, P.C., Russell, C., Nesic, Z., Lee, X., Chen, S.G., Staebler, R., Novak, M.D., 1996. Annual cycles of water vapour and carbon dioxide fluxes in and above a boreal aspen forest. Global Change Biol. 2 (3), 219–229.

Bowling, D.R., Baldocchi, D.D., Monson, R.K., 1999. Dynamics of isotopic exchange of carbon dioxide in a Tennessee deciduous forest. Global Biogeochem. Cycles 13 (4), 903–922.

Bowling, D.R., Tans, P.P., Monson, R.K., 2001. Partitioning net ecosystem carbon exchange with isotopic fluxes of CO_2. Global Change Biol. 7 (2), 127–145.

Bowling, D.R., McDowell, N.G., Bond, B.J., Law, B.E., Ehleringer, J.R., 2002. C-13 content of ecosystem respiration is linked to precipitation and vapor pressure deficit. Oecologia 131 (1), 113–124.

Bowling, D.R., Pataki, D.E., Ehleringer, J.R., 2003a. Critical evaluation of micrometeorological methods for measuring ecosystem-atmosphere isotopic exchange of CO_2. Agric. Forest Meteorol. 116 (3–4), 159–179.

Bowling, D.R., Sargent, S.D., Tanner, B.D., Ehleringer, J.R., 2003b. Tunable diode laser absorption spectroscopy for stable isotope studies of ecosystem-atmosphere CO_2 exchange. Agric. Forest Meteorol. 118 (1–2), 1–19.

Buchmann, N., Ehleringer, J.R., 1998. CO_2 concentration profiles, and carbon and oxygen isotopes in C-3, and C-4 crop canopies. Agric. Forest Meteorol. 89 (1), 45–58.

Buchmann, N., Brooks, J.R., Flagagan, L.B., Ehleringer, J.R., 1998. Carbon isotope discrimination of terrestrial ecosystems. In: Griffiths, H. (Ed.), Stable Isotopes. BIOS Science, Oxford, UK, pp. 203–221.

Dang, Q.L., Margolis, H.A., Sy, M., Coyea, M.R., Collatz, G.J., Walthall, C.L., 1997. Profiles of photosynthetically active radiation, nitrogen and photosynthetic capacity in the boreal forest: implications for scaling from leaf to canopy. J. Geophys. Res.-Atmos. 102 (D24), 28845–28859.

DuMouchel, W., O'Brien, F., 1989. Integrating a robust option into a multiple regression computing environment. In: Berk, K., Malone, L. (Eds.), Computing Science and Statistics: Proceedings of the 21st Symposium on the Interface, American Statistical Association, Alexandria, VA, pp. 297–301.

Duranceau, M., Ghashghaie, J., Badeck, F., Deleens, E., Cornic, G., 1999. Delta C-13 of CO_2 respired in the dark in relation to delta C-13 of leaf carbohydrates in *Phaseolus vulgaris* L.-under progressive drought. Plant Cell Environ. 22 (5), 515–523.

Ehleringer, J.R., Buchmann, N., Flanagan, B., 2000. Carbon isotope ratios in belowground carbon cycle processes. Ecol. Appl. 10 (2), 412–422.

Farquhar, G.D., Ehleringer, J.R., Hubick, K.T., 1989. Carbon isotope discrimination and photosynthesis. Annu. Rev. Physiol. Plant Mol. Biol. 40, 503–537.

Fessenden, J.E., Ehleringer, J.R., 2003. Temporal variation in delta C-13 of ecosystem respiration in the Pacific Northwest: links to moisture stress. Oecologia 136 (1), 129–136.

Field, C.B., Mooney, H.A., 1986. The photosynthesis-nitrogen relationship in wild plants. In: Givnish, T.J. (Ed.), On the Economy of Plant Form and Function. Cambridge University Press, New York, pp. 25–55.

Flanagan, L.B., Brooks, J.R., Varney, G.T., Berry, S.C., Ehleringer, J.R., 1996. Carbon isotope discrimination during photosynthesis and the isotope ratio of respired CO_2 in boreal forest ecosystems. Global Biogeochem. Cycles 10 (4), 629–640.

Flanagan, L.B., Ehleringer, J.R., 1998. Ecosystem-atmosphere CO_2 exchange: interpreting signals of change using stable isotope ratios. Trends Ecol. Evol. 13 (1), 10–14.

Flanagan, L.B., Kubien, D.S., Ehleringer, J.R., 1999. Spatial and temporal variation in the carbon and oxygen stable isotope ratio of respired CO_2 in a boreal forest ecosystem. Tellus Ser. B-Chem. Phys. Meteorol. 51 (2), 367–384.

Fung, I., Field, C.B., Berry, J.A., Thompson, M.V., Randerson, J.T., Malmstrom, C.M., Vitousek, P.M., Collatz, G.J., Sellers, P.J., Randall, D.A., Denning, A.S., Badeck, F., John, J., 1997. Carbon 13 exchanges between the atmosphere and biosphere. Global Biogeochem. Cycles 11 (4), 507–533.

Ghashghaie, J., Duranceau, M., Badeck, F.W., Cornic, G., Adeline, M.T., Deleens, E., 2001. Delta C-13 of CO_2 respired in the dark in relation to delta C-13 of leaf metabolites: comparison between *Nicotiana sylvestris* and *Helianthus annuus* under drought. Plant Cell Environ. 24 (5), 505–515.

Goulden, M.L., Daube, B.C., Fan, S.M., Sutton, D.J., Bazzaz, A., Munger, J.W., Wofsy, S.C., 1997. Physiological responses of a black spruce forest to weather. J. Geophys. Res.-Atmos. 102 (D24), 28987–28996.

Griffis, T.J., Baker, J.M., Sargent, S., Tanner, B.D., Zhang, J., 2004a. Measuring field-scale isotopic CO_2 fluxes using tunable diode laser absorption spectroscopy and micrometeorological techniques. Agric. Forest Meteorol. 124, 15–29.

Griffis, T.J., Black, T.A., Gaumont-Guay, D., Drewitt, G.B., Nesic, Z., Barr, A.G., Morgenstern, K., Kljun, N., 2004b. Seasonal variation and partitioning of ecosystem respiration in a southern boreal aspen forest. Agric. Forest Meteorol. 125, 207–223.

Griffis, T.J., Lee, X., Baker, J.M., King, J.Y., Sargent, S.D., 2005. Feasibility of quantifying ecosystem-atmosphere C18O16O fluxes and discrimination mechanisms using laser spectroscopy. Agric. Forest Meteorol., submitted for publication.

Henn, M.R., Chapela, I.H., 2000. Differential C isotope discrimination by fungi during decomposition of C_3- and C_4-derived sucrose. Appl. Environ. Microbiol. 66 (10), 4180–4186.

Högberg, P., Nordgren, A., Buchmann, N., Taylor, A.F.S., Ekblad, A., Högberg, M.N., Nyberg, G., Ottosson-Lofvenius, M., Read, D.J., 2001. Large-scale forest girdling shows that current photosynthesis drives soil respiration. Nature 411 (6839), 789–792.

Keeling, C.D., 1958. The concentration and isotopic abundances of atmospheric carbon dioxide in rural areas. Geochim. Cosmochim. Acta 13, 322–334.

Klumpp, K., Schäufele, R., Lötscher, M., Lattanzi, F.A., Feneis, W., Schnyder, H., 2005. C-isotope composition of CO_2 respired by shoots and roots: fractionation during dark respiration? Plant Cell Environ. 28, 241–250.

Knohl, A., Werner, R.A., Brand, W.A., Buchmann, N., 2005. Short-term variations in $d^{13}C$ of ecosystem respiration reveals link between assimilation and respiration in a deciduous forest. Oecologia 142, 70–82.

Lai, C.T., Schauer, A.J., Owensby, C., Ham, J.M., Ehleringer, J.R., 2003. Isotopic air sampling in a tallgrass prairie to partition net ecosystem CO_2 exchange. J. Geophys. Res.-Atmos. 108 (D18), 456610.1029/2002JD003369.

Lai, C.T., Ehleringer, J.R., Tans, P., Wofsy, S.C., Urbanski, S.P., Hollinger, Y., 2004. Estimating photosynthetic ^{13}C discrimination in terrestrial CO_2 exchange from canopy to regional scales. Global Biogeochem. Cycles 18, GB104110.1029/2003GB002148.

Lee, X., Sargent, S., Smith, R., Tanner, B., 2005. In-situ measurement of water vapor isotopes for atmospheric and ecological applications. J. Atmos. Oceanic Technol. 22, 555–565.

Leff, B., Ramankutty, N., Foley, J.A., 2004. Geographic distribution of major crops across the world. Global Biogeochem. Cycles 18, GB100910.1029/2003GB002108.

Lin, G.H., Ehleringer, J.R., 1997. Carbon isotopic fractionation does not occur during dark respiration in C-3 and C-4. Plant Physiol. 114 (1), 391–394.

Lloyd, J., Farquhar, G.D., 1994. ^{13}C discrimination during CO_2 assimilation by the terrestrial biosphere. Oecologia 99, 201–215.

Lloyd, J., Kruijt, B., Hollinger, D.Y., Grace, J., Francey, R.J., Wong, S.C., Kelliher, F.M., Miranda, A.C., Farquhar, G.D., Gash, J.H.C., Vygodskaya, N.N., Wright, I.R., Miranda, H.S., Schulze, E.D., 1996. Vegetation effects on the isotopic composition of

atmospheric CO_2 at local and regional scales: theoretical aspects and a comparison between rain forest in amazonia and a boreal forest in Siberia. Aust. J. Plant Physiol. 23 (3), 371–399.

Marschner, F.J., 1974. The original vegetation of Minnesota, U.S. Department of Agriculture, Forest Service. North Central Forest Experiment Station, St. Paul, MN. Redraft of the original 1930 edition.

McDowell, N.G., Bowling, D.R., Bond, B.J., Irvine, J., Law, B.E., Anthoni, P., Ehleringer, J.R., 2004. Response of the carbon isotopic content of ecosystem, leaf, and soil respiration to meteorological and physiological driving factors in a *Pinus ponderosa* ecosystem. Global Biogeochem. Cycles 18 (1), GB101310.1029/2003GB002049.

Morgenstern K., Black T.A., Humpreys E.R., Griffis T.J., Cai T., Drewitt G.B., Gaumont-Gnay D., Nesic Z., 2004. Sensitivity and uncertainty of the carbon balance of a Pacific Northwest Douglas-fir forest during El Niño/La Niño cycle. Agric. forest Meteorol. 123, 201–219.

Ogée, J., Peylin, P., Ciais, P., Bariac, T., Brunet, Y., Berbigier, P., Roche, C., Richard, P., Bardoux, G., Bonnefond, J.M., 2003. Partitioning net ecosystem carbon exchange into net assimilation and respiration using (CO_2)-C-13 measurements: a cost-effective sampling strategy. Global Biogeochem. Cycles 17 (2) 1070, doi: 10.1029/2002GB001995.

Ogée, J.P., Peylin, P., Cuntz, M., Bariac, T., Brunet, Y., Berbigier, P., Richard, P., Ciais, P., 2004. Partitioning net ecosystem carbon exchange into net assimilation and respiration with canopy-scale isotopic measurements: An error propagation analysis with $^{13}CO_2$ and $CO^{18}O$ data. Global Biogeochem. Cycles, 18 (2) GB2019, doi: 10.1029/2003GB002166.

Ometto, J.P.H.B., Flanagan, L.B., Martinelli, L.A., Moreira, M.Z., Higuchi, N., Ehleringer, J.R., 2002. Carbon isotope discrimination in forest and pasture ecosystems of the Amazon Basin, Brazil. Global Biogeochem. Cycles 16 (4), 110910.1029/2001GB001462.

Pataki, D.E., Ehleringer, J.R., Flanagan, L.B., Yakir, D., Bowling, D.R., Still, C.J., Buchmann, N., Kaplan, J.O., Berry, J.A., 2003. The application and interpretation of Keeling plots in terrestrial carbon cycle research. Global Biogeochem. Cycles 17 (1), 102210.1029/2001GB001850.

Price, D.T., Black, T.A., 1990. Effects of short-term variation in weather on diurnal canopy CO_2 flux and evapotranspiration of a juvenile Douglas-fir stand. Agric. Forest Meteorol. 50, 139–148.

Randerson, J.T., Still, C.J., Balle, J.J., Fung, I.Y., Doney, S.C., Tans, P.P., Conway, T.J., White, J.W.C., Vaughn, B., Suits, N., Denning, A.S., 2002. Carbon isotope discrimination of arctic and boreal biomes inferred from remote atmospheric measurements and a biosphere-atmosphere model. Global Biogeochem. Cycles 16 (3), 102810.1029/2001GB001435.

Raupach, M.R., Finnigan, J.J., 1998. Single-layer models of evaporation from plant canopies are incorrect but useful, whereas multilayer models are correct but useless. Aust. J. Plant Physiol. 15, 705–716.

Riley, W.J., Still, C.J., Torn, M.S., Berry, J.A., 2002. A mechanistic model of (H_2O)-O-18 and (COO)-O-18 fluxes between ecosystems and the atmosphere: model description and sensitivity analyses. Global Biogeochem. Cycles 16 (4), 1095–1109.

Rochette, P., Flanagan, L.B., Gregorich, E.G., 1999. Separating soil respiration into plant and soil components using analyses of the natural abundance of carbon-13. Soil Sci. Soc. Am. 63, 1207–1213.

Schotanus, P., Nieuwstadt, F.T.M., De Bruin, H.A.R., 1983. Temperature measurement with a sonic anemometer and its application to heat and moisture fluxes. Boundary Layer Meteorol. 26, 81–93.

Vogel, J.C., 1980. Fractionation of the carbon isotopes during photosynthesis. Sitzungsberichte der Heidelberger Akademie der Wissenschaften Mathematisch-naturwissenschaftliche Klasse Jahrgang. Berlin, Springer-Verlag, pp. 111–135.

Wang, Y.P., Leuning, R., 1998. A two-leaf model for canopy conductance, photosynthesis, and partitioning available energy. I. Model description. Agric. Forest Meteorol. 91, 89–111.

Webb, E.K., Pearman, G.I., Leuning, R., 1980. Corrections of flux measurements for density effects due to heat and water vapour transfer. Quar. J. R. Meteorol. Soc. 106, 85–100.

Yakir, D., Sternberg, L.D.L., 2000. The use of stable isotopes to study ecosystem gas exchange. Oecologia 123 (3), 297–311.

Yakir, D., Wang, X.F., 1996. Fluxes of CO_2 and water fluxes between terrestrial vegetation and the atmosphere estimated from isotope measurements. Nature 380, 515–517.

Zhang, J., Griffis, T.J., Baker, J.M., 2005. Using continuous stable isotope measurements to partition net ecosystem CO_2 exchange into photosynthesis and respiration of a corn–soybean rotation ecosystem. Plant Cell Environ., in press.